Transition Analysis as a Solution for Fragmentary Remains: Estimating Age-at-Death for a Skeletal Collection from Gurat, France

by

Laurel McInnis

A thesis
presented to the University of Waterloo
in fulfillment of the
thesis requirement for the degree of
Masters of Arts
in
Public Issues Anthropology

Waterloo, Ontario, Canada, 2022

Author's Declaration

I hereby declare that I am the sole author of this thesis. This is a true copy of the thesis, including any required final revisions, as accepted by my examiners.

I understand that my thesis may be made electronically available to the public.

Abstract

Transition Analysis is an age-at-death estimation method developed in 2002. While originally developed using the same skeletal features as other methods, Transition Analysis was recently expanded to include121 features from across the skeleton. This makes Transition Analysis a potential solution for cases where common age-at-death estimation sites are missing or damaged. In this study, eight of the individuals from the Gurat skeletal collection are aged using Transition Analysis. The individuals were also aged using traditional age-at-death estimation methods for comparative purposes. Finally, the individuals were aged using only the lower limbs to simulate a challenging recovery scenario. The goal of this study was to promote Transition Analysis as an option for age-at-death estimation in cases of fragmentary remains and varied preservation within a collection. The results of the study show that Transition Analysis can estimate age in cases where traditional methods are not applicable. Transition Analysis is also able to estimate age-at-death using just the lower limbs. However, the results were extremely imprecise. This study found Transition Analysis to be a promising but imperfect solution to estimating age-at-death for fragmentary skeletal remains.

Acknowledgments

I would like to thank my supervisor, Dr. Maria Liston, for her support and guidance during what has been an unusual sixteen months. I am grateful I had the opportunity to work with and learn from her. I would also like to thank Dr. Alexis Dolphin for allowing me to work on the Gurat skeletal collection on such short notice. I would also like to thank Dr. Dolphin for agreeing to serve on my committee. Additionally, I would like to thank my third committee member, Dr. Bonnie Glencross, for her time and effort in reviewing my thesis.

I am grateful to Dr. Michael Gervers for the time and care he took excavating the Gurat site and the dedication he gave to studying the materials.

Thank you to my professors, Dr. Adrienne Lo, Dr. Jennifer Liu, Dr. Alexis Dolphin, and Dr. Maria Liston, for their guidance and aid in preparing me during the first two semesters of the program,

I would also like to thank my parents, Karen and John, for their patience and support during this time. Thank you also to my friends, Maddie and Isabella and my roommate, Louie the cat, for keeping my spirits up.

I would like to thank my graduate cohort for their encouragement and advice. In particular I would like to thank Grace Chan for her companionship and academic advice during our time in the lab and after.

Finally, thank you to the people of Gurat. I will be forever grateful for the opportunity to learn from you.

Table of Contents

List of Figures vi

List of Tables vii

Chapter 1 1

1.2 Changes Due to COVID-19 .... *1*

1.3 Public Issues *2*

1.4 Age-at-Death Estimation from Fragmentary Remains *3*

1.5 The Gurat Collection *4*

1.6 Proposed Venue of Publication *7*

Chapter 2 8

2.1 Introduction *8*

2.1.1 History of the Gurat Collection 8

2.1.2 Age-at-Death Estimation 9

2.1.3 Development of Transition Analysis 12

2.2 Materials and Methods *15*

2.2.1 Selecting a Sample 15

2.2.2 Data Collection 15

2.3 Results *18*

2.4 Discussion *23*

2.5 Conclusion *28*

References 30

Appendix A: 34

Appendix B: 50

Appendix C: 52

List of Figures

Figure 1: Results from TA3 using the entire skeleton 20

Figure 2: Results from TA3 using just the lower limbs 22

Figure 3: Comparison of age-at-death results from the entire skeleton and just the lower limbs 23

List of Tables

Table 1: Traits that should be excluded from TA3 analysis 16

Table 2: Traits scored differently between first and second scoring 17

Table 3: Results from TA3 analysis using the entire skeleton 19

Table 4: Number of traits scored compared to the prediction interval (entire skeleton) 19

Table 5: Results from TA3 analysis using just the lower limbs 21

Table 6: Number of traits scored compared to the prediction interval (lower limbs only) 21

Table 7: Number of scorable traits by region 24

Chapter 1
The Church of St. George and Public Issues Anthropology

1.1 Introduction

Age is one of the most fundamental aspects of the human identity and bioarchaeologists spend a great deal of time and effort trying to estimate the age of a person from their skeleton. One of the major challenges in adult age-at-death estimation is the loss of key analytical sites on the bones through the fragmentation of the skeleton. In 2002, a new age-at-death estimation method, Transition Analysis, was introduced. This method was updated in 2019. The aim of my research is to determine if Transition Analysis is a viable solution to adult age-at-death estimation in cases of fragmentary remains. Additionally, I wanted to see if Transition Analysis could perform in a particularly challenging fragmentation scenario: the preservation of only the lower limbs. This research problem was originally developed for a skeletal population from Thebes, Greece, but travel restrictions due to COVID-19 prevented me from accessing this collection. Instead, the research problem was adapted for application to Gurat, France skeletal collection.

1.2 Changes Due to COVID-19

Before discussing my research, it is important to outline how the COVID-19 pandemic has affected it. My original research question involved using Transition Analysis to produce age-at-death estimates for a skeletal population from Thebes, Greece. The Thebes collection comes from an excavation of the Ismenion Hill directed by Stephanie Larson and Kevin Daly of Bucknell University (Daly & Larson et al., 2011-2015). The Ismenion Hill area was used as a cemetery beginning in the 4th century CE. Although there is no documentary evidence, the high rates of pathology, particularly leprosy, suggest that the site was associated with a hospice or hospital (Liston, 2018).

As previously mentioned, the most widely used methods for age-at-death estimation rely on the skull and pelvis. The Ismenion Hill graves were used for multiple inhumations and were later partially excavated, leaving mostly legs and feet behind (Liston, 2018). These conditions made the Ismenion Hill collection an ideal candidate for Transition Analysis. As Transition Analysis uses a variety of traits from across the skeleton, a collection comprised of mostly legs and feet is a viable candidate for the method. This was the topic of my original thesis: using Transition Analysis to produce age-at-death estimates on the Ismenion Hill collection as traditional methods could not be used. However, the Ismenion Hill collection is housed in the Wiener Laboratory of the American School of Classical Studies in Athens, Greece (Liston, 2021). The COVID-19 pandemic made travel impossible, and I could not use the Ismenion Hill population for my research. Fortunately, Dr. Alexis Dolphin allowed me access to her research materials, the Gurat collection, and I was able to adapt my research to fit the new materials.

1.3 Public Issues

In order to discuss how my research classifies as public issues anthropology, it is necessary to first define the term. Broadly, public issues anthropology can be defined as "the application of anthropological knowledge, techniques, and epistemology beyond university and college settings to the public domain" (Hedican, 2016, p. 80). This definition reflects the ultimate goals of public issues anthropology: to move away from the "ivory tower" model of anthropology and stop treating the public as outsiders to anthropological research (Grima, 2016).

In public issues anthropology, the “public” refers to both the holders of public interest and public policy (the state) and the general public (Richardson & Almansa-Sánchez, 2015).

There is no standard model of public issues anthropology that can be applied to all research: the way in which the public can be meaningfully engaged is unique to each subfield, geographic region, and research project (Grima, 2016). Because of this, it is the responsibility of each individual researcher to do their work using the framework of public issues. Ultimately, the goal of public issues anthropology is to conduct research for the benefit of the public and, when possible, with the cooperation of the public.

1.4 Age-at-Death Estimation from Fragmentary Remains

Age-at-death estimation is one of the first steps done in any skeletal analysis. In bioarchaeology, age-at-death provides insight into the lived experience of the individual (Martin, Harrod, and Pérez, 2013). In forensic archaeology, it is a fundamental piece of demographic information that can lead to the identification of the individual (Franklin, 2009). The ability to produce accurate age-at-death estimates relies on the use of reliable methods. The most reliable and widely used methods for adult age-at-death estimation require the pelvis and the skull to be present and well-preserved (Martin, Harrod, and Pérez, 2013).

Over time, decomposition will affect all bone. The rate of decomposition is determined by extrinsic factors, such as soil acidity, and intrinsic factors, such as bone density (Marado, Braga, and Fontes, 2018). Additionally, looting adds uncertainty to which skeletal elements will be present upon excavation (Martin, Harrod, and Pérez, 2013). However, it is not only the preservation of the bone itself that is necessary: the individual features on the bones must be present for age-at-death estimation to be possible. In the case of the pelvis, the pubic symphysis and the auricular surface are the most reliable and commonly used sites for adult age-at-death estimation. Both the pubic symphysis and the auricular surface have a multi-decade history of use in bioarchaeology (Todd, 1920; Lovejoy et al., 1985). However, a case study conducted at the Windover site in Florida determined that within the pelvis, the pubis is the least likely to be preserved (Stojanowski, Seidemann, and Doran, 2002). This means that archaeologists must be prepared to draw upon a variety of less reliable and well-established age-at-death estimation methods in case the required elements are not well preserved.

Transition Analysis, a statistical age-at-death estimation method developed in 2002, attempts to present a solution to this problem. While Transition Analysis was developed using the common methods that require the presence of the skull and pelvis, it has since been updated to incorporate 121 skeletal traits from across the body (Getz, 2020). Transition Analysis presents a solution to age-at-death estimation without the skull or pelvis. Therefore, the use of Transition Analysis potentially will serve to prepare bioarchaeologists more thoroughly for cases of fragmentary skeletal remains. The Gurat skeletal collection is one such case. Some individuals in the Gurat skeletal collection are preserved well while others are badly fragmented and pose significant analytical difficulty (Meijer, 2018). My research applies Transition Analysis in this manner and promotes it as an option for age-at-death estimation in cases of fragmentary remains, particularly in cases where traditional age-at-death estimation methods are difficult or impossible to apply.

1.5 The Gurat Collection

The Gurat skeletal collection was excavated from the Church of St. George, a cave-church in southwestern France. The excavation of the site, which was directed by Veronika and

Michael Gervers, began in 1965 and concluded in the mid-1970s (Meijer et al., 2019). The Gurat collection is currently housed in the Ancient and Contemporary Environmental Bioindicators Laboratory (ACEBioLab) at the University of Waterloo under the supervision of Dr. Alexis Dolphin. The collection consists of eighteen individuals, eight of which are suitable for my research. The other ten individuals are either subadults or too fragmentary for macroscopic study.

The Gurat site contains evidence of long-term occupation. Among the materials excavated from the site were several coins; the earliest coin dates the site to 1237-1286CE and the latest coin dates it to 1655-1701 CE. Additionally, charcoal from a pottery fragment found in grave Hb produced a radiocarbon date of 1390 CE (Franklin & Gervers, 1978). These dates represent the minimum period of occupation as the site may have been in use before or after the deposition of the artefacts. Although only eighteen individuals were excavated from the site, it is estimated that approximately 200 more individuals may remain buried (Meijer et al., 2019). The time-depth of the site combined with the low proportion of the cemetery represented in the collection makes it impossible to determine if the collection is a single group or several different groups.

The Gurat skeletal collection is interesting because although there are only a few publications analyzing the remains, the collection has been extensively studied. Unpublished research stored with the collection shows that osteobiographies have been produced by at least two separate research teams (Gaherty et al., 1978; Clements & Gruspier, n.d.). Additionally, several calcanei were borrowed for an adult body weight estimation study in 1972 and never returned nor was the study published (Seymour, 2019). Research notes and rough drafts of the two osteaobiographical studies are housed in the ACEBioLab with the skeletal collection.

Although the studies produced useful information about the Gurat skeletal collection, the information is only accessible to those who have access to the lab.

Unpublished research is not open for criticism, alternative interpretations of data, or academic scrutiny. It does not undergo the review process that is required for publication in a peer-reviewed journal: this is the process that affirms research and adds it to the scientific record (Allen, 2014). Researchers also have a duty to publish because that is how findings become accessible to the public. Publication is a key part of the evolution of scientific knowledge: it is through publication that new information is added to the body of knowledge (Singhal & Kalra, 2021). If one's research is not published, it is not available to either the academic public or the general public. This duty to publish is explicitly discussed in the Society for American Archaeology's ethics statement. The statement says that knowledge gained from the archaeological record must be presented to the public (by academic publication or other means) and deposited in a suitable place for safekeeping (Society for American Archaeology, 1996). The publication of research is clearly an important aspect of responsible science and a duty researchers have both to the public and to each other. Through this thesis, I am both bringing the unpublished research done on the Gurat skeletal collection to the public and contributing to the knowledge of the site.

Locally, the church of St. George is not well understood. Before the excavations began in 1965, the residents in the area did not pay much attention to the site: the church was used as a garbage dump for many years (Seymour, 2019). Additionally, there is no reference to any subterranean church in the local archives (Gervers, 1967). Despite the lack of local awareness of the site, it has been there for nearly a millennium (Franklin & Gervers, 1978). The church of St. George is an important part of the history of Gurat and the people who live in the area have a right to knowledge of their history. Therefore, research into the history and occupation of the church of St. George is an important public issue. My research is relevant to public issues anthropology because I will be studying a major source of evidence about the use of the church of St. George: the skeletons. As UWSpace is open access, my research will be fully available to any person who has an interest in the Gurat site and will contribute to the available information about the site and its occupants.

1.6 Proposed Venue of Publication

My proposed venue of publication for this research is The American Journal of Biological Anthropology (AJBA). This journal publishes a wide variety of anthropological research within the areas of bioarchaeology, paleoanthropology, skeletal biology, genetics, human biology, and non-human primates including research in new and developing areas (American Journal of Physical Anthropology, 2021). As my research focusses on age-at-death estimation, it is appropriate for publication in this journal. This journal has previously published articles on Transition Analysis, including a validation study by two of the developers of the method (Milner & Boldsen, 2012). Through its previous publication of Transition Analysis research, the AJBA has demonstrated that Transition Analysis is of interest to its editors and is appropriate for publication in this journal. Additionally, the AJBA is the leading publication in biological anthropology and has a wide reach. As my research has both archaeological and forensic implications, a publication with a diverse readership, such as the AJBA, is ideal.

Chapter 2
Transition Analysis as a Solution for Fragmentary Remains: Estimating Age-at-Death for a Skeletal Collection from Gurat, France

2.1 Introduction

2.1.1 History of the Gurat Collection

The cave church of Gurat, from which the Gurat skeletal collection was excavated, is in southwestern France. Local archival records make no reference to the church, but it is referred to locally as the Church of St. George (Gervers, 1967). The Church of St. George is one of many subterranean churches in the Charente region of France, likely due to the predominance of sedimentary rock in the area (Gervers, 1967). Under the direction of Dr. Michael Gervers, excavation of the site began in 1965 and concluded in the mid-1970s (Meijer et al., 2019). Coins excavated from the site give evidence for the period of occupation: the earliest date is between 1237-1286 CE while the latest date is between 1655-1701. A radiocarbon date of 1390 CE produced from a piece of charcoal falls within the range indicated by the numismatic evidence (Franklin & Gervers, 1978). The occupation of the site coincides with a period of great instability in Europe: the 14th century saw France ravaged by both the Hundred Years War with England and several waves of the Black Death. As the church of St. George is situated on two Medieval pilgrimage routes, the site has been identified as a likely site for group hermetism (Meijer, 2018).

The 1966 excavation season revealed fragments of human bones buried at the church (Gervers, 1967). The excavated remains belong to 18 individuals in varying states of fragmentation (Seymour, 2019). The site was never fully excavated, and it has been estimated that approximately 200 individuals remain buried beneath the church of St. George (Meijer et al., 2019). Because of the long period of occupation and the incomplete nature of the excavations, it cannot be determined if the excavated individuals belonged to a single population group or if they represent a series of population groups who occupied the site over time (Meijer, 2018). Because of this uncertainty, I will refer to the skeletons as the Gurat skeletal collection and will not define the collection as a population.

2.1.2 Age-at-Death Estimation

Age is one of the most fundamental aspects of human identity; it is a key piece of demographic data upon which many other aspects of bioarchaeology are built. In addition to communicating how old a person is, age is an important aspect of one's social identity. Age can determine what behaviours are appropriate, what responsibilities one has to the group, and one's social status within the group (Sofaer, 2011). However, age is not a simple concept. In life, age generally refers to the number of years that have elapsed since birth. In bioarchaeology, demographic data is rarely available, and the skeleton serves as the primary source of evidence for a person's biological profile. By studying the skeleton, researchers can produce a biological age. Biological age is the physical age of the body as a result of the formation and subsequent degeneration of the body. In bioarchaeology, biological age is used as a proxy for chronological age (Couoh, 2017). Unfortunately, the relationship between biological and chronological age is complicated by the interference of factors other than age that impact the skeleton. In particular, sex, genetics, nutrition, pathology, and biomechanical factors impact the appearance of the bones. Up to 60% of variation in skeletal age indicators can be associated with factors other than age (Mays, 2015).

Biological age is primarily expressed in the skeleton first by growth and then by senescence. Because degeneration is more variable and affected by environmental factors than growth, subadult age-at-death estimation is usually more accurate than adult age-at-death estimation (Franklin, 2010). Adult age-at-death estimation is focussed on skeletal traits that senesce in consistent ways. The two main traits are both located on the pelvis: the pubic symphysis and the auricular surface. The pubic symphyseal face, the point at which the two pubic bones connect, undergoes changes in texture over the life course. Todd systematically documented these changes using the Hamann-Todd collection and produced an age-at-death estimation method based on the appearance of the pubic symphyseal surface (Todd, 1920). This method was redeveloped on a different skeletal collection in 1990. The original Todd pubic symphysis method showed unusually high peaks at certain five-year intervals. Todd explained this as the result of ages being rounded up in the demographic records. Brooks restudied the same collection and suggested alternative morphological features and a shift in the associated age ranges. This new pubic symphysis method is generally referred to as the Suchey-Brooks method (Brooks & Suchey, 1990). The other trait that is commonly used for adult age-at-death estimation is the auricular surface. The auricular surface is the point of articulation between the ilium and the sacrum. It was first developed into an age-at-death estimation method in 1985 (Lovejoy et al., 1985). The method was revised by Buckberry and Chamberlain to evaluate different features of the auricular surface independently of each other. The auricular surface is of particular interest because it has higher rates of survival and discovery than the pubic symphysis (Buckberry & Chamberlain, 2002).

Although adult ageing is primarily expressed through the senescence of the skeleton, there are features that continue to develop into adulthood. One such trait is the sternal epiphysis of the clavicle. The sternal epiphysis of the clavicle is characterized by its late fusion relative to the other major epiphyses: it generally does not begin fusing until twenty-one and may not complete until twenty-eight (Stevenson, 1924). An individual with an unfused sternal epiphysis is most likely under the age of twenty-eight. The other developmental adult age-at-death estimation method is cranial suture closure. Cranial suture closure has been in use for centuries but was discounted in the mid-1900s due to its unreliability (Brooks, 1955). It was revisited by Meindl and Lovejoy in 1985 and their standards for age-at-death estimation using cranial suture closure are still in use today. The researchers identified 7 vault sutures and 5 lateral-anterior sutures that are of particular interest and specified that all sutures must be ectocranial. Their system for recording closure is scored on a scale of 0-3 from fully open to completely obliterated (Meindl & Lovejoy, 1985).

As adult age-at-death estimation is heavily reliant on a few key areas of the skeleton, it can be difficult or impossible to produce estimates for fragmented remains. However, it is common, particularly in archaeological settings, for remains to be fragmentary (Passalacqua, 2013). One of the areas of the skeleton on which it is difficult to perform age-at-death analysis is the lower limbs. Changes in the trabeculae of the proximal femur occur in a relatively uniform manner and can be used to estimate age-at-death. Arthritic changes, specifically those associated with osteoarthritis, can also be used to estimate age-at-death. However, arthritic changes are heavily influenced by factors such as sex and lifestyle. It is more appropriate to use arthritic changes as a way to establish the upper and lower boundaries of age within a population (Priya, 2017). Another age-at-death estimation method that be applied to the lower limbs is bone histology. Bone histology is the study of changes in the microstructure of bones, often with a particular focus on remodelling activity. Midshaft cross sections of the tibia, fibula, or femur can be analyzed to produce an age-at-death estimate (Streeter, 2012). Although bone histology shows great potential for age-at-death estimation in cases where only the lower limbs are present, it is an inherently destructive technique and requires specialized training and equipment, making it less accessible than other age-at-death estimation.

2.1.3 Development of Transition Analysis

Transition Analysis is a statistical approach to adult age-at-death estimation that was introduced in 2002. The method calculates the probability of a skeleton transitioning from one stage to the next, thus the name Transition Analysis. It was created to address four key issues in age-at-death estimation: (1) how to best represent uncertainty in age-at-death estimation, a problem usually addressed through the use of discrete age categories; (2) how to avoid age mimicry, an occurrence where the age distribution of the research population mimics the distribution of the reference population on which the method was developed; (3) how to best combine multiple skeletal indicators, something for which there is no accepted standard; and (4) how to score anatomical features in a way that captures morphological variation, particularly morphological features that have multiple separate age-related changes associated with them, such as the auricular surface (Boldsen et al., 2002). In order to address these issues, the method is based on Bayesian statistics rather than regression analysis. Regression analysis is the statistical process for estimating the relationship between an independent variable and a dependant variable. In contrast, Bayesian statistics loosens the relationship between the independent and dependant variables by supplementing the data with a prior probability distribution. In Transition Analysis, the prior probability distribution takes the form of a uniform prior: a skeletal collection of known ages to inform the software of an expected distribution of ages in a skeletal population. Transition Analysis derives its uniform prior from 17th century Danish parish records (Milner & Boldsen, 2012). The loosened relationship between the variables in Bayesian statistics was first established as a solution to age mimicry in bioarchaeology a decade before the development of Transition Analysis (Konigsberg & Frankenberg, 1992).

One of the key features of Transition Analysis is that the results are probabilistically tailored to each individual; it does not assign individuals to pre-existing age-at-death categories but rather it creates a unique maximum likelihood age and associated confidence interval for each individual (Getz, 2019). This is in contrast to traditional, phase-based methods where every individual in a specific phase is assumed to have the same degree of error. At the time of the original publication, Transition Analysis utilized 19 skeletal traits from three areas: the pubic symphysis, the auricular surface, and the ectocranial surface. Although the traits used in Transition Analysis are based on the same key areas as traditional methods, the traits found in those areas as scored independently rather than as a group in order to capture the most morphological variation (Boldsen et al., 2002). The original version of Transition Analysis was developed using the Terry Collection and the Coimbra Identified Skeletons Collection. The second version of Transition Analysis used the same skeletal traits and did not involve additional research on skeletal collections of known age (Milner & Boldsen, 2012). Transition Analysis was made available through a downloadable computer program in which users could input the expression of the observed skeletal traits based on an attached scoring manual. The program would then produce a maximum likelihood estimate for age-at-death along with a 95% confidence range (Getz, 2020).

The latest version of Transition Analysis, Transition Analysis 3 (TA3) was introduced in 2019. The development team collected data on features from more than 1600 skeletons from the United States, Portugal, South Africa, and Thailand, including collections from the University of

Tennessee and the Museum of London. This was done to ensure that regional and ancestry-relation variation was accounted for in the method (Ousley et al., 2019). The updated method increased the number of scorable traits from the original 19 to 121. In TA3, the scorable traits are located across the skeleton, meaning that the method no longer relies exclusively on the skull and pelvis (Getz, 2020). In this way, TA3 is more distinct from traditional age-at-death methods than previous versions of Transition Analysis. The pelvis still has the largest number of scorable traits, followed closely by the vertebral column (Milner et al., 2019). When both sides of a bilateral trait are scored, the software will only use the right side in its analysis. In TA3, age-at-death estimation results are presented in the form of a maximum likelihood estimate, an upper 95% precision bound, a lower 95% precision bound, and a standard error (Milner et al., 2020). TA3 is available as a downloadable software. The software has the statistical package built-in, making the method accessible to bioarchaeologists who do not have a strong statistical background (Milner et al., 2020).

Since the publication of TA3, Transition Analysis has become a potential solution for cases of skeletal fragmentation for two reasons: its adaptability and its distribution of traits. Because each trait in Transition Analysis is assessed separately in the software, not every trait needs to be scored in order for an age-at-death estimate to be produced (Milner & Boldsen, 2012). This is particularly true of TA3: the high number of scorable traits means the exclusion of non-scorable traits will not have a grave impact on the results. In this way, TA3 can be used adaptively to suit the particular skeleton and its fragmentation. Additionally, the use of traits distributed across the body in TA3 allows for age-at-death estimates to be produced even for incomplete skeletons (Ousley et al., 2019). This is particularly useful in cases where the bones used in traditional age-at-death estimation are absent or damaged.

2.2 Materials and Methods

2.2.1 Selecting a Sample

Prior to my research, the Gurat skeletal collection had already been cleaned, sorted, and labelled (Clements & Gruspier, n.d.). The collection is currently stored in carboard boxes and housed in the Ancient and Contemporary Environmental Bioindicators Laboratory (ACEBioLab) at the University of Waterloo. The Gurat skeletal collection is comprised of 18 individuals. TA3 is based on adult-age-at death estimation traits and in order for the software to produce an estimate, a minimum of two traits must be scored (Milner et al., 2020). A minimum of two traits are required in order for the statistical software to run. In order to qualify for my sample, an individual had to be an adult and have at least two scorable traits. The subadults in the collection had already been identified and labelled by Gaherty et al. (1978) and a skeletal inventory had already been taken for all individuals (Seymour, 2019). As a result, sample selection was a very straightforward process. Eight individuals qualified for my sample: GU 1, GU 2, GU 3, GU 7, GU 8, GU 9, GU 11, and GU 12.

2.2.2 Data Collection

To begin, the TA3 software, user guide, trait manual, and data collection form from https://www.statsmachine.net/software/TA3/ was downloaded. The format of the provided data collection form was cramped and difficult for me to read. To ensure data collection went as smoothly as possible, I developed my own data collection forms in Microsoft Excel using the information from the provided form. Since the publication of the TA3 software, the developers have identified several traits that should be left out of any analysis (Table 1). Most of the identified traits are recommended for exclusion due to not contributing to analysis while diffuse idiopathic skeletal hyperostosis (DISH) shows evidence of selective mortality and will may bias the results (Milner et al., 2020). As some of the traits recommended for exclusion are bilateral and DISH is scored on the cervical, thoracic, and lumbar vertebra, the total number of traits that should be excluded was 16. This brought the number of scorable traits down from 121 to 105. All of these traits were excluded from my data collection form and my analysis.

Trait	**Reason for Exclusion**
DISH	Selective mortality
Fibula wings	Not informative
Ischial spur	Not informative
R1 fusion	Not informative
Radius tuberosity crest	Not informative
Sacral elbow	Not informative
Ulna olecranon spur	Not informative

Table 1: Traits that should be excluded from TA3 analysis (Adapted from Milner et al., 2020)

The traits used by TA3 are divided into three categories: descriptive traits, traits with non-metric thresholds, and traits with metric thresholds. I scored the traits based on the descriptions and photographs included in the trait scoring manual. A lamp was used to assist in the scoring of traits involving surface texture. Metric traits were measured using dial calipers. All skeletons were scored twice to reduce intra-observer error. Table 2 shows the number of traits scored differently between the first and second scoring. The variation was low enough that a third scoring was not required. For all skeletons, the second scoring was used because I was more confident in my observations after having gained experience with the method. Once data collection was complete, the data collected from the second scoring was put into the TA3 software using the procedures in the user guide (Milner et al, 2020).

Individual	No. of Traits Different Between First and Second Scoring
GU 1	1
GU 2	4
GU 3	2
GU 7	5
GU 8	2
GU 9	2
GU 10	1
GU 11	0

Table 2: Traits scored differently between first and second scoring

I also performed traditional age-at-death estimation on my sample. I scored the skeletons using the Meindl and Lovejoy cranial suture closure method (1985), the Buckberry and Chamberlain auricular surface method (2002), and the Suchey-Brooks pubic symphysis method (Brooks & Suchey, 1990). I followed the standards for these methods as described by Buikstra and Ubelaker (1994). After scoring, I compared results from the three methods and assigned each individual to either the early adult (20-34 years), middle adult (35-49 years), or late adult (50+ years) category as a way of combining the results. These age categories were taken from Buikstra and Ubelaker (1994). Individuals were sorted into a category based on where the age-at-death results from the three methods were concentrated.

Finally, I ran the collected TA3 data through the software again, this time only including traits from the lower limbs. I did this to test how TA3 would perform in a situation with challenging skeletal preservation. Including bilateral traits, the lower limbs have 12 scorable traits in TA3. This was a blind study: no other research conducted on the Gurat skeletal collection was read until after data collection was completed.

2.3 Results

TA3 produce age-at-death estimation results for all 8 individuals in my sample. These results were produced by running the software with every observed trait for each individual. Appendix A contains the data collection forms for the entire sample and shows which traits were scored for each individual. TA3 produces both a maximum likelihood estimate for age-at-death and an upper and lower 95% prediction bound. The maximum likelihood estimate is the point estimate of the 95% prediction interval: it is not an exact age-at-death estimation. For simplicity, I will refer to the maximum likelihood estimates as age-at-death estimates with the understanding that they cannot be responsibly separated from their prediction interval.

TA3 provides both a prediction interval and a standard error. I will be using the prediction interval, which is defined by the upper and lower bounds, and not the standard error when discussing the produced age-at-death estimates. In a normal statistical distribution, the standard error will account for approximately 68% of variability. This level of accuracy is not high enough to draw meaningful conclusion from age-at-death estimation. The 95% prediction interval is less precise but more accurate than the standard error. However, the 95% prediction interval is generally too wide to provide meaningful age-at-death estimates.

Table 3 shows the results from TA3. The age-at-death estimates for the individuals of my sample range from 28.2 to 63.2 years of age. There is a large difference between the smallest prediction interval, GU 3, and the largest, GU 12. Table 4 shows the relationship between the number of traits scored and the size of the prediction interval. In both Table 3 and Table 4, GU 3, GU 8, GU 9, and GU 1 are the first four individuals listed. This shows that the four youngest individuals have the four smallest prediction intervals. Figure 1 shows the age-at-death estimates and associated prediction intervals for all individuals. The chart visualizes how much smaller the prediction intervals are for the younger individuals in the sample.

ID	Estimated Age	Lower 95% Prediction Bound	Upper 95% Prediction Bound	Standard Error
GU 3	28.2	18.0	38.1	9.9
GU 8	32.3	16.9	47.3	10.5
GU 9	33.3	20.6	46.1	9.3
GU 1	52.9	34.5	70.5	9.1
GU 11	58.0	36.0	81.1	10.0
GU 7	59.2	40.1	77.5	8.4
GU 2	61.1	41.5	80.1	8.5
GU 12	63.2	37.1	90.2	12.5

Table 3: Results from TA3 analysis using the entire skeleton

ID	No. of Traits Scored	Prediction Interval
GU 3	39	20.1
GU 9	41	25.5
GU 8	22	30.4
GU 1	71	36.0
GU 7	62	37.4
GU 2	97	38.6
GU 11	11	45.1
GU 12	4	53.1

Table 4: Number of traits scored compared to the prediction interval (entire skeleton)

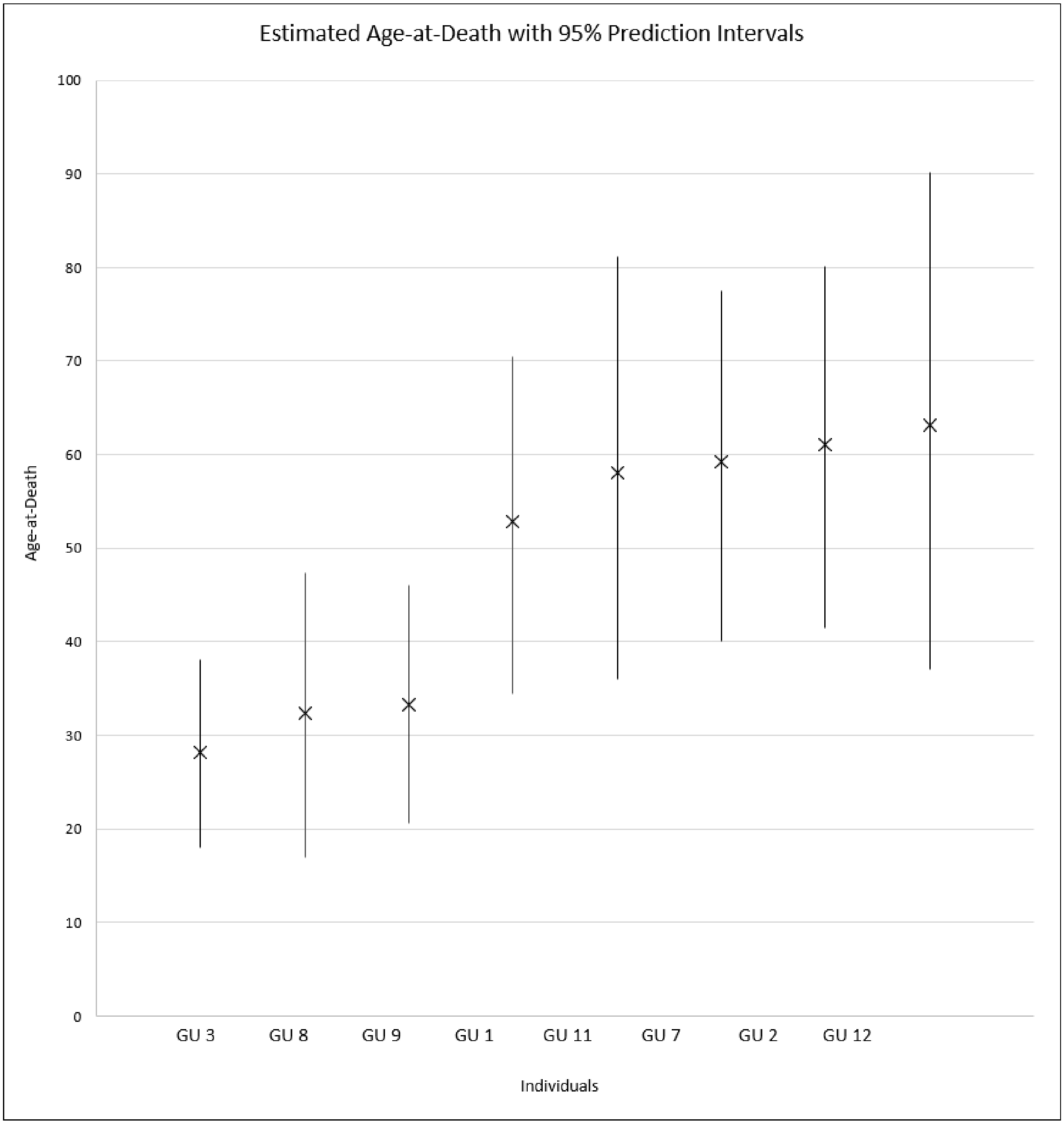

Figure 1: Results from TA3 using the entire skeleton

The fragmentation of my sample made it difficult to perform traditional age-at-death estimation. Six of the 8 individuals had scorable auricular surfaces. Two of the 8 individuals had scorable pubic symphyses. Five of the 8 individuals had a preserved cranium. The cranial sutures on the skull vault consistently estimated the individuals to be significantly younger than the methods from the pelvis. Damage to the lateral-anterior portion of the skulls of GU 3, GU 8, and

GU 9 made it impossible to score all the sutures required to produce an age-at-death estimation. After combining the data, all scorable individuals but GU 3 were classified as being in the middle adult category. GU 3 was classified as an early adult. GU 12 had no preserved age-at-death estimation sites and could not be scored.

Transition Analysis was also performed on the sample using just the lower limbs. GU 12 was excluded some the sample as the individual had no scorable lower limbs. Table 5 shows the results from the analysis using just the lower limbs. The age-at-death in this analysis ranged from 38.5 to 75.3 years of age. Table 6 shows that the lower limb analysis did not involve many traits. It also shows that the prediction intervals from this analysis were extremely large. No meaningful interpretation can be made from such imprecise age-at-death estimates. The prediction intervals from just the lower limbs were consistently larger than the prediction intervals from the entire skeleton (Figure 2).

ID	Estimated Age	Lower 95% Prediction Bound	Upper 95% Prediction Bound	Standard Error
GU 8	38.5	16.6	61.0	11.9
GU 3	39.1	9.5	68.4	14.9
GU 9	46.9	23.3	71.6	11.6
GU 2	57.0	32.4	82.6	11.6
GU 1	60.7	36.1	86.0	11.6
GU 11	67.9	42.6	92.9	11.9
GU 7	75.3	52.4	97.3	12.1
GU 12	n/a	n/a	n/a	n/a

Table 5: results from TA3 analysis using just the lower limbs

ID	No. of Traits Scored	Prediction Interval
GU 8	5	44.4
GU 7	9	44.9
GU 9	11	48.3
GU 1	10	49.9
GU 2	11	50.2
GU 11	5	50.3
GU 3	4	58.9
GU 12	n/a	n/a

Table 6: Number of traits scored compared to the prediction interval (lower limbs only)

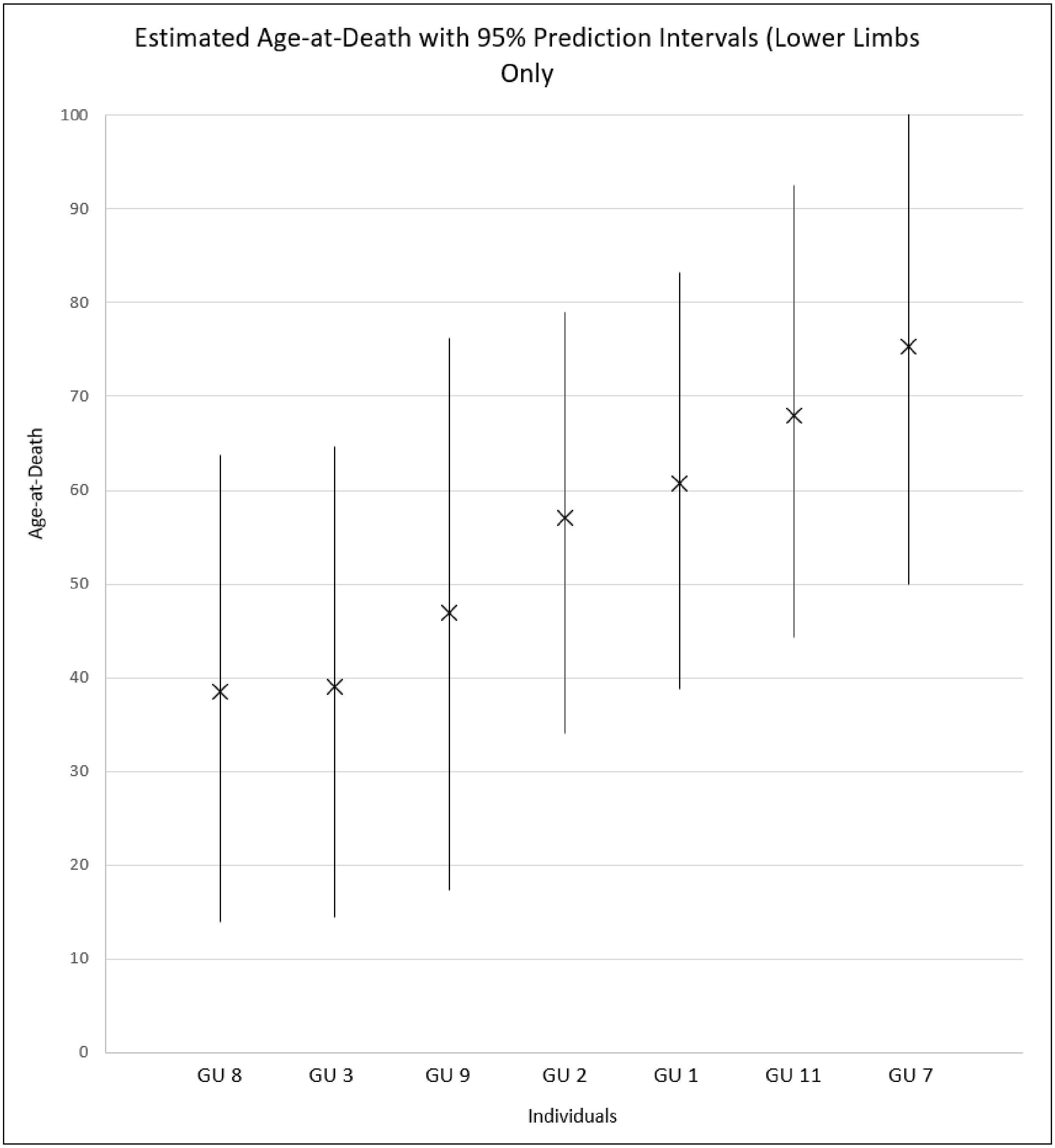

Figure 2: Results from TA3 using just the lower limbs

In both the full skeletal analysis and the lower limb analysis, GU 3, GU 8, and GU 9 are noticeably younger than the other individuals. With the exception of GU 2, the age-at-death of the individuals were consistently older in the lower limb analysis (Figure 3).

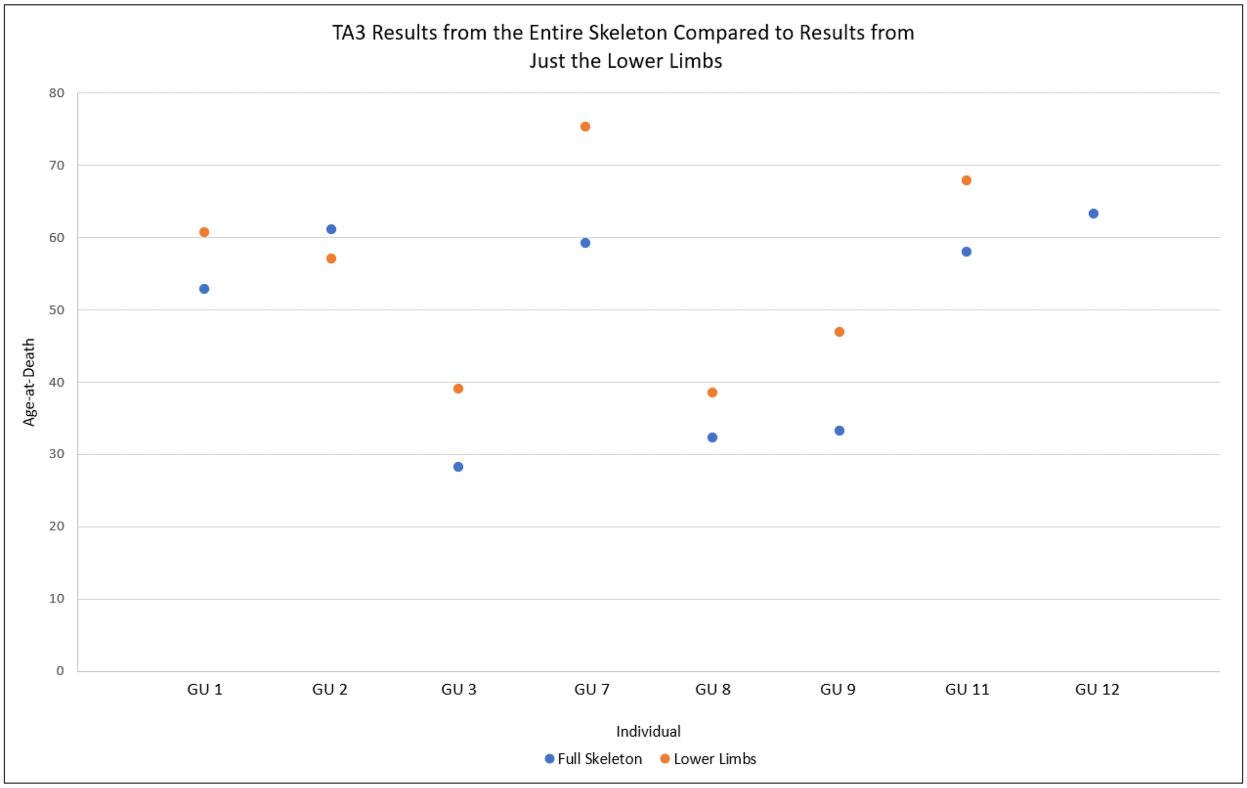

Figure 3: Comparison of age-at-death results from the entire skeleton and just the lower limbs

Traditional age-at-death estimation could be performed on 7 of the 8 individuals: GU 12 was too fragmentary to be scored using any traditional method. Due to the fragmentation of the skeletons, only two individuals, GU 2 and GU 7, could be aged using all three methods: none of the other individuals had undamaged pubic symphyses. The cranial vault sutures consistently aged the skeletons younger than the auricular surface, pubic symphysis, and lateral-anterior sutures.

2.4 Discussion

The results of the full skeleton TA3 analysis on the Gurat skeletal collection varied in their precision. One of the individuals, GU 3, had a prediction interval of 20.1 years while another, GU 12, had a prediction interval of more than fifty years. Such a wide prediction interval makes it nearly impossible to draw any meaningful conclusions about the age of the individual as the interval covers nearly the entire lifespan. For most of the individuals, the prediction interval covers a significant portion of both middle adulthood and late adulthood (Table 3). The results from the entire skeleton are not sufficiently precise to contribute to research on the lived experiences of the individuals. There is some connection between the age-at-death of the individual and the size of the prediction interval: the four youngest individuals, GU 3, GU 8, GU 9, and GU 1, had the smallest prediction intervals. This connection is not observable in the older individuals.

The number of traits scored does not affect the size of the prediction interval in the same way age-at-death does. The youngest individuals do not have the greatest number of traits scored (Table 4). It is possible that there is some connection between the number of traits scored and the prediction interval. Table 4 shows that the individuals with the largest prediction intervals, GU 11 and GU 12, had the fewest number of traits scored by a large amount. It is possible that there is a threshold for the number of traits scored under which precision greatly decreases. Further study would be required to determine if this is the case.

Region	**No. of Scorable Traits**
Cranium	5
Vertebral Column	25
Ribs and Sternum	10
Clavicle and Scapula	10
Upper Limbs	17
Pelvis	40
Lower Limbs	14

Table 7: Number of scorable traits by region

Age-at-death was also estimated using just the lower limbs in order to simulate a challenging recovery scenario. GU 12 was excluded from the sample as the individual had no scorable lower limbs preserved due to fragmentation. The maximum number of traits that can be scored using the lower limbs is twelve (Table 7). The specific traits scored for each region can be found on the data collection forms included in Appendix A. As previously mentioned, there appears to be a connection between a low number of scorable traits and low precision. This connection also appears in the TA3 analysis using just the lower limbs: all 7 of the individuals included in the lower limb analysis have a prediction interval of larger than forty years. The size of the prediction intervals means that the age-at-death estimates for all 7 individuals are essentially meaningless. A forty year range covers more than half of the adult lifespan and limits the amount of information that can be interpreted from the results.

As previously mentioned, the Gurat skeletal collection is not known to be a single population of people. Therefore, it is inappropriate to treat them as if they are a single population. What the results do show is that despite the large prediction interval, the results of TA3 using just the lower limbs can still give insight into the ages of the individuals in relation to each other. Figure 2 demonstrates that despite the overlapping prediction intervals, GU 7 is likely older than GU 8, GU 3, and GU 9. These results are similar to the results from the entire skeleton. By looking at the most likely ages without the prediction intervals, the results show that the results from the lower limbs are not drastically different than the results from the entire skeleton (Figure 3). Figure 3 also shows that the results from the lower limbs, with the exception of GU 2, are consistently older than the results from the entire skeleton. This suggests that the traits found on the lower limbs produce older age-at-death results. A possible explanation for this is the influence of factors other than age on the skeletal traits. As the lower limbs are weight bearing, they may be more prone to bony changes due to activity-related changes or arthritic changes. The reliability of age-related features on the lower limbs warrants further study.

I used the Buckberry and Chamberlain auricular surface phase method, the Suchey-Brooks pubic symphysis method, and the Meindl and Lovejoy cranial suture closure method to estimate the ages of the skeletons in addition to TA3. There is no accepted standard within bioarchaeology for combining multiple age indicators: it is commonly done on a case-by-case basis and is based on the researcher's personal experience (Garvin, 2012). In order to combine the results in this study, the results from the three methods were compared. Age-at-death categories were assigned based on the concentration of results. In cases where the pelvic results disagreed with the cranial results, more weight was put on the pelvic results due to the fragmentation of many of the skulls (Appendix B). GU 3 had unfused sternal epiphyses on both clavicles, so they were classified as an early adult. The other 6 scorable individuals were classified as middle adults based on the method results. As the different method results do not fully agree with each other, it is possible that a different researcher could age the individuals differently by comparing the age indicators in a different way. TA3 takes the choice of the researcher out of multifactorial age-at-death estimation. The traits scored in TA3 are all scored independently within the software and then weighted and combined to produce the age-at-death results. This has the potential to reduce interobserver error in age-at-death estimation and ensure accuracy.

One of the issues Transition Analysis was developed to address was how to best represent uncertainty in age-at-death estimation. In traditional age-at-death estimation methods, this is done using discrete age categories. Often, the final age category is a terminal category, such as fifty and above. This serves to mask variation: every individual within a category is equally likely to be every individual age within the category. Additionally, the use of terminal age categories results in elderly individuals being essentially invisible. Although the wide prediction intervals may prevent meaningful analysis of the collection, the use of a most likely age-at-death and a prediction interval results in a unique result for each individual. Five of the 8 individuals in the Gurat skeletal collection were estimated to be over fifty years of age based on the most likely age-at-death. Using traditional age categories, all 5 individuals would be homogenized as 50+ while TA3 indicates that both GU 2 and GU 3 are likely to be in the sixth decade of life.

The descriptions and photographs included in the documentation of the method make TA3 extremely user friendly. The traits are easy to identify, and the scoring system is extremely clear. The only exception to this is the weight-related traits. The humerus, tibia, calcaneus, and innominate all possess a trait where the researcher must score the bone as either normal or light to identify age-related bone loss. These traits are scored based on the researcher's judgement and there is no information in the documentation on the expected weight of the bones due to variation related to sex, stature, and lifestyle factors (Milner et al., 2019). As a researcher with fair amount of experience handling archaeological remains, I have very rarely interacted with these bones unaffected by either taphonomy or trauma. Therefore, I was not confident in my ability to differentiate between a normal bone and a light bone.

Because TA3 combines the age indicators in the software and does not rely on the researchers to do so, the method is extremely friendly to less experienced researchers. As previously mentioned, the majority of bioarchaeologists combine multiple age indicators based primarily on their experience. As a researcher who has been trained to analyze bones but who has not conducted a large amount of independent research, I feel ill prepared to make such judgement calls.

2.5 Conclusion

Overall, TA3 did not perform as well as I had hoped. The results from the entire skeleton were varied in their usefulness: some of the individuals had small prediction intervals and their age-at-death estimations could be used for interpretive analysis while others had too broad a prediction interval to be very informative. However, the ability for TA3 to produce age-at-death estimates beyond age 50 is a notable improvement on traditional methods. The presence of older adults within the Gurat skeletal collection is likely given the results.

The usefulness of the method significantly reduced when it was applied only to the lower limbs. While TA3 is potentially a useful alternative to other age-at-death estimation methods, its most interesting feature is its ability to be applied to cases of challenging fragmentation. Unfortunately, the lower limbs do not have enough traits for TA3 to produce results that are precise enough for interpretation. At best, the results from the lower limbs can be used to show the ages of the individuals in relation to one another. If a researcher had a population that was not suitable for other age-at-death estimation, TA3 could be used to identify individuals as being either in the upper or lower age range of the population. Although not ideal, this application of TA3 is better than having no age-at-death information at all.

Transition Analysis has addressed several issues in adult age-at-death estimation, such as age mimicry and terminal age categories. However, it is not a marked improvement on the accuracy and precision of traditional age-at-death estimation methods when the pelvis is available. For many of the individuals in the Gurat skeletal collection, the TA3 results would not be conducive to further study: no meaningful interpretation can be derived from age-at-death results that cover several decades. Instead, Transition Analysis finds its niche in providing age-at-death estimation in cases where other methods cannot be used. It was not useful in the case of the lower limbs, but it was able to results when other methods could not. I would not recommend using TA3 to estimate age-at-death using just the lower limbs. However, there are other areas of the skeleton that may be more useful. In particular, the vertebral column has twenty-five scorable traits, over twice as many as the lower limbs (Table 7). The upper limbs may also be an area of interest. Further study on the usefulness of TA3 in cases of fragmentation should focus on isolating areas of the skeleton and testing the precision and accuracy of the method on just those regions. This type of study has the potential to determine which types of fragmentation have the most potential use for TA3 in its current state.

Although TA3 cannot yet provide precise age-at-death estimates using only the lower limbs, the inclusion of traits from across the skeleton only began in 2019. If the developers of Transition Analysis continue to focus on expanding the method to estimate age-at-death using non-traditional traits, TA3 could become an invaluable tool for researchers faced with fragmentary remains.

References

Allen, M. (2014). Ethics in the Publishing of Archaeology. In C. Gnecco & D. Lippert (Eds.), *Ethics and Archaeological Praxis* (pp. 185-199). Springer. https://doi.org/10.1007/978-1-4939-1646-7

American Journal of Biological Anthropology. (2021). *Author Guidelines.* Retrieved May 18, 2021, from https://onlinelibrary.wiley.com/page/journal/10968644/homepage/forauthors.html

Boldsen, J. L., Milner, G. R., Konigsberg, L. W., and Wood, J. W. (2002). Transition Analysis: A New Method for Estimating Age from Skeletons. In R. D. Hoppa & J. W. Vaupel (Eds.), *Paleodemography: Age Distributions from Skeletal Samples* (pp. 73-106). Cambridge University Press. https://doi:10.1017/CBO9780511542428.005.

Brooks, S., & Suchey, J. M. (1990). Skeletal age determination based on the os pubis: A comparison of the Acsádi-Nemeskéri and Suchey-Brooks methods. *Human Evolution*, *5*(3), 227-238. https://doi.org/10.1007/BF02437238

Brooks, S.T. (1955). Skeletal age at death: The reliability of cranial and pubic age indicators. *American Journal of Physical Anthropology 13*, 567-589.

Buckberry, J. L. & Chamberlain, A. T. (2002). Age Estimation From the Auricular Surface of the Ilium: A Revised Method. *American Journal of Physical Anthropology, 119,* 231-239.

Buikstra, J. E. & Ubelaker, D. H. (1994). *Standards for Data Collection from Human Skeletal Remains: Proceedings of a Seminar at The Field Museum of Natural History.* Arkansas Archaeological Survey Research Series No. 44.

Clements, V. & Gruspier, K. (n.d.) An Analysis of Skeletal Material from the Rock-Cut Church at Gurat. Unpublished.

Couoh, L. R. (2017). Differences between biological and chronological age-at-death in human skeletal remains: A change of perspective. American Journal of Physical Anthropology 163, 671-695. https://doi.org/10.1002/ajpa.23236

Daly, K, and Stephanie L. et al. (2011-2015) "Archaeological Investigations in the Area of the Ismenion and Herakleion Sanctuaries of Thebes." Unpublished reports to the Hellenic Ministry of Culture and Sport.

Franklin, D. (2010). Forensic age estimation in human skeletal remains: Current concepts and future directions. *Legal Medicine, 12*(1), 1-7. https://doi.org/10.1016/j.legalmed.2009.09.001

Franklin, U. M. & Gervers, M. (1978). The Technical Analysis of Coinage from the Medieval Rock-Cut Church at Gurat, France. *Journal of the International Institute for Conservation – Canadian Group, 3*(2), 2-6.

Gaherty, G., Gretenhart, C. E. C., & Gretenhart, F. H. (1978). Skeletal Remains from a Medieval Cemetery, Gurat, Charente. Unpublished manuscript.

Gervers, M. (1967). The Cave Church at Gurat (Charente): Preliminary Report. *Gesta, 6*, 10-20.

Garvin, H. M., and Passalacqua, N. V. (2012). Current Practices by Forensic Anthropologists in Adult Skeletal Age Estimation. *Journal of Forensic Sciences 57*(2), 427-433. https://doi.org/10.1111/j.1556-4029.2011.01979.x

Getz, S. M. (2019). *The Use and Misuse of Transition Analysis: An Assessment of the Boldsen et al. Age-at-Death Estimation Method.* Proceedings of the American Academy of Forensic Science, 71st Annual Scientific Meeting, Baltimore.

Getz, S. M. (2020). The use of Transition Analysis in skeletal age estimation. *WIREs Forensic Science*, *2*(6), e1378. https://doi.org/10.1002/wfs2.1378

Grima, R. (2016). But Isn't All Archaeology 'Public' Archaeology? *Public Archaeology, 15*(1), 50-58. https://doi.org/10.1080/14655187.2016.1200350

Hedican, E. J. (2016). *Public Anthropology: Engaging Social Issues in the Modern World.* University of Toronto Press: North York, Ontario.

Konigsberg, L. W. & Frankenberg S. R. (1992). Estimation of Age Structure in Anthropological Demography. American Journal of Physical Anthropology, 89(2), 235-256.

Liston, M. (2018). *Inferring the presence of a leprosarium or hospital from the pathologies in the cemetery: Interpreting burials from Byzantine Thebes.* Paper presented at the 19th International Congress of Classical Archaeology, Germany.

Liston, M. 2021. Personal Communication. Waterloo, ON. University of Waterloo.

Lovejoy, C. O., Meindl, R. S., Pryzbeck, T. R., and Mensforth, R. P. (1985). Chronological Metamorphosis of the Auricular Surface of the Ilium: A New Method for the Determination of Adult Skeletal Age at Death. *American Journal of Physical Anthropology 68*, 15-28.

Marado, L. M., Braga, C., & Fontes, L. (2018). Bone diagenesis in Via XVII inhumations (Bracara Augusta): Identification of taphonomic and environmental factors in differential skeletal preservation. *Estudos do Quaternário, 18*, 67-76.

Martin, D., Harrod, R. P., & Ventura, R. (2013). *Bioarchaeology: An Integrated Approach to Working with Human Remains.* Springer: New York.

Mays, S. (2015). The effect of factors other than age upon skeletal age indicators in the adult. *Annals of Human Biology, 42*(4), 332-341. https://doi.org/10.3109/03014460.2015.1044470

Meijer, J. (2018). *Exploring the Origins and Mobility of the Medieval Monastic Inhabitants of a Cave Church in Gurat, France using Strontium Isotope Analysis* [Master's thesis, University of Waterloo]. UWSpace.

Meijer, J., Dolphin, A. E., Yakymchuk, C., & Gervers, M. (2019). Interpreting medieval mobility from burials at the rock-hewn church of St. Georges, Gurat (France): Insights from strontium isotope analysis of bones and teeth. *International Journal of Osteoarchaeology*, 574-583. https://doi.org/10.1002/oa.2753

Meindl, R. S. & Lovejoy, C. O. (1985). Ectocranial Suture Closure: A Revised Method for the Determination of Skeletal Age at Death Based on the Lateral-Anterior Sutures. *American Journal of Physical Anthropology 68*, 57-66.

Milner, G. R., & Boldsen, J. L. (2012). Transition Analysis: A validation study with known-age modern American skeletons. *American Journal of Physical Anthropology, 148*(1), 98-110. https://doi.org/10.1002/ajpa.22047

Milner, G. R., Boldsen, J. L., Ousley, S. D., Getz, S. M., Weise, S., & Tarp P. (2019). *Transition Analysis 3 (TA3) Trait Manual. Public Distribution Ver. 1.*

Milner, G. R., Boldsen, J. L., Ousley, S. D., Getz, S. M., Weise, S., & Tarp P. (2020). *TA3 Installation and Software User Guide: Version 0.16.*

Ousley, S. D., Milner, G. R., Boldsen, J. L., Getz, S. M., & Weise, S. (2019). *A New Method for Adult Age Estimation Using Transition Analysis: TA3.* Proceedings of the American Academy of Forensic Science, 71st Annual Scientific Meeting, Baltimore.

Passalacqua, N. V. (2013). Subadult Age-at-Death Estimation from the Human Calcaneus. *International Journal of Osteoarchaeology, 23*, 471-474.

Priya, E. (2017). Methods of skeletal age estimation used by forensic anthropology in adults: a review. *Forensic Research & Criminology International Journal*, *4*(2), 41-51.

Richardson, L., & Almansa-Sánchez, J. (2015). Do you even know what public archaeology is? Trends, theory, practise, ethics. *World Archaeology*, *47*(2), 194-211. http://dx.doi.org/10.1080/00438243.2015.1017599

Seymour, G. (2019). *Reconstructing the Life Histories of the Individuals Buried in the Rock-cut Cave Church of St. Georges, in Gurat, France* [Master's thesis, University of Waterloo]. UWSpace.

Singhal, S., & Kalra, B. S. (2021). Publication ethics: Role and responsibility of authors. *Indian Journal of Gastroenterology*, *40*(1), 65–71. https://doi.org/10.1007/s12664-020-01129-5

Society for American Archaeology. (1996). *Principles of Archaeological Ethics*. Retrieved September 15, 2021. https://www.saa.org/career-practice/ethics-in-professional-archaeology

Sofaer, J. (2011). Towards a Social Bioarchaeology of Age. In S. C. Agarwal & B. A. Glencross (Eds.), *Social Bioarchaeology* (pp. 285-311). Wiley-Blackwell.

Stojanowski, C. M., Seidemann, R. M., & Doran, G. H. (2002). Differential Skeletal Preservation at Windover Pond: Causes and Consequences. *American Journal of Physical Anthropology*, *119*, 15-26. https://doi.org/10.1002/ajpa.10101

Streeter, M. (2012). Histological Age-at-Death Estimation. In C. Crowder & S. Stout (Eds.), *Bone Histology: An Anthropological Perspective* (pp. 135-152). CRC Press.

Todd, T. W. (1920) Age changes in the pubic bone. I. The white male pubis. *American Journal of Physical Anthropology 3*(3), 285-334. https://doi.org/10.1002/ajpa.1330030301

White, T. D. and Folkens, P. A. (2005). *The Human Bone Manual*. Elsevier Academic Press.

Appendix A:

Collection GURAT ID# GRAVE HA / GU 1

Notes auricular surface is present bilaterally
neither pubic symphysis remains
only 4 sternal rib ends.
cranial vault is broken and glued together – sutures are observable but obscured.

Cranium	Left / Midline					Right		
parietal depression	**abs**	pres				**abs**	pres	
spheno-occipital synch.	open	close						
occipital condyle lipping	abs	>50%	>75%			abs	>50%	>75%

Vertebral Column	Midline					
C1 lipping	**abs**	>50%				
C1 eburnation	**abs**	pres				
L1 spinuous process	round	flat	ossif			
L1 superior body surface	NF	PF	RL	**FF**	GF	**flat**
L1 inferior body surface	NF	PF	RL	**FF**	GF	**flat**
L5 superior margin	round	sharp	lipped			
L5 inferior margin	round	sharp	lipped			
L5 superior body surface	NF	PF	RL	**FF**	GF	**flat**
L5 inferior body surface	NF	PF	RL	**FF**	GF	**flat**
S1 margin	**round**	sharp	lipped			
S1-2 fusion	**>1cm**	<1cm	close			
cervical lipping	abs	**>3mm**			# scorable = 3	
thoracic lipping	**abs**	>3mm			# scorable = 10	
lumbar lipping	**abs**	>3mm			# scorable = 5	
cervical candlewax	**abs**	pres				
thoracic candlewax	**abs**	pres				
lumbar candlewax	**abs**	pres				

Sternum and Ribs	Left / All						Right
sternum dorsal ridge	abs	pres					
R2 rim profile	regular	irreg	abs	cone	claw	both	
R3-10 rim profile	**regular**	irreg	**abs**	cone	claw	both	
R2 shingle rib	norm	shingle					
R3-10 shingle ribs	norm	shingle					

Clavicle / Scapula	Left				Right			
medial epiphysis fusion	NF	PF	RL	**FF**	NF	PF	RL	**FF**
medial epiphysis gravel	**abs**	pres			**abs**	pres		
medial macroporosity	**abs**	>3	many		**abs**	>3	many	
lateral macroporosity	**abs**	>3			**abs**	>3		
glenoid fossa lipping	**abs**	<1/2	>1/2		abs	**<1/2**	>1/2	

Humerus	Left / All				Right			
humerus weight	normal	light						
lesser tubercle bumps	abs	>1/3			abs	>1/3		
lesser tubercle margin	round	raised	lipped		round	raised	lipped	
greater tubercle pits	abs	pres			abs	pres		
medial epicondyle	smth	rough			smth	rough		
lateral epicondyl	smth	rough			smth	rough		
Trapezium	Left				Right			
trapezium lipping	abs	>2mm			abs	>2mm		
Femur	Left				Right			
fovea margin lipping	abs	>10mm			abs	>10mm		
head surface	smth	>5mm	>10mm		smth	>5mm	>10mm	
gr. trochanter roughening	abs	tri	rec	OH	abs	tri	rec	OH
trochanteric fossa exostos	abs	pres			abs	pres		
trochanteric medial exostos	abs	pres			abs	pres		
Tibia / Fibula / Calcaneus	Left / All				Right			
tibia weight	normal	light			normal	light		
calcaneus weight	normal	light			normal	light		
Inominates	Left / All				Right			
inominate weight	normal	light						
SI joint fusion	abs	fused	SA		abs	fused	SA	
iliac crest fusion	NF	PF	RL	FF	NF	PF	RL	FF
ilium tuberculum ossif	abs	ossif	db ossif		abs	ossif	db ossif	
ant. Inf. iliac spine exostos	abs	>75%			abs	>75%		
acetabulum margin lipping	abs	>10mm			abs	>10mm		
acetabulum post. surface	smth	rough			smth	rough		
acetabulum inf. end lipping	abs	>3mm			abs	>3mm		
isch. tuberosity bumps	abs	<50%	>50%		abs	<50%	>50%	
Sacroiliac Joint	Left				Right			
inferior surface porosity	abs	porosity			abs	porosity		
sup. posterior iliac exostos	smth	exos			smth	exos		
inf. posterior iliac exostos	smth	exos			smth	exos		
posterior exostos	smth	discont	cont		smth	discont	cont	
Pubic Symphysis	Left				Right			
pubic symphyseal collar	abs	collar			abs	collar		
symphyseal relief	billows	resid	flat		billows	resid	flat	
superior protuberance	serrat	knob	flat		serrat	knob	flat	
ventral margin	serrat	ramp	rim	BD	serrat	ramp	rim	BD
dorsal margin	serrat	ramp	rim	BD	serrat	ramp	rim	BD

Collection	GURAT	ID#	GRAVE HB / GU2

Notes
X 2nd analysis

Cranium	Left / Midline					Right			
parietal depression	abs	pres				abs	pres		
spheno-occipital synch.	open	close							
occipital condyle lipping	abs	>50%	>75%			abs	>50%	>75%	
Vertebral Column	**Midline**								
C1 lipping	abs	>50%							
C1 eburnation	abs	pres							
L1 spinuous process	round	flat	ossif						
L1 superior body surface	NF	PF	RL	FF	GF	flat			
L1 inferior body surface	NF	PF	RL	FF	GF	flat			
L5 superior margin	round	sharp	lipped						
L5 inferior margin	round	sharp	lipped						
L5 superior body surface	NF	PF	RL	FF	GF	flat			
L5 inferior body surface	NF	PF	RL	FF	GF	flat			
S1 margin	round	sharp	lipped						
S1-2 fusion	>1cm	<1cm	close						
cervical lipping	abs	>3mm			# 4				
thoracic lipping	abs	>3mm			# 5				
lumbar lipping	abs	>3mm			# 5				
cervical candlewax	abs	pres							
thoracic candlewax	abs	pres							
lumbar candlewax	abs	pres							
Sternum and Ribs	**Left / All**					**Right**			
sternum dorsal ridge	abs	pres							
R2 rim profile	regular	irreg	abs	cone	claw	both			
R3-10 rim profile	regular	irreg	abs	cone	claw	both			
R2 shingle rib	norm	shingle							
R3-10 shingle ribs	norm	shingle							
Clavicle / Scapula	**Left**					**Right**			
medial epiphysis fusion	NF	PF	RL	FF		NF	PF	RL	FF
medial epiphysis gravel	abs	pres				abs	pres		
medial macroporosity	abs	>3	many			abs	>3	many	
lateral macroporosity	abs	>3				abs	>3		
glenoid fossa lipping	abs	<1/2	>1/2			abs	<1/2	>1/2	

Humerus	Left / All				Right			
humerus weight	normal	light						
lesser tubercle bumps	abs	>1/3			abs	>1/3		
lesser tubercle margin	round	raised	lipped		round	raised	lipped	
greater tubercle pits	abs	pres			abs	pres		
medial epicondyle	smth	rough			smth	rough		
lateral epicondyl	smth	rough			smth	rough		

Trapezium	Left				Right			
trapezium lipping	abs	>2mm			abs	>2mm		

Femur	Left				Right			
fovea margin lipping	abs	>10mm			abs	>10mm		
head surface	smth	>5mm	>10mm		smth	>5mm	>10mm	
gr. trochanter roughening	abs	tri	rec	OH	abs	tri	rec	OH
trochanteric fossa exostos	abs	pres			abs	pres		
trochanteric medial exostos	abs	pres			abs	pres		

Tibia / Fibula / Calcaneus	Left / All				Right			
tibia weight	normal	light			normal	light		
calcaneus weight	normal	light			normal	light		

Inominates	Left / All				Right			
inominate weight	normal	light						
SI joint fusion	abs	fused	SA		abs	fused	SA	
iliac crest fusion	NF	PF	RL	FF	NF	PF	RL	FF
ilium tuberculum ossif	abs	ossif	db ossif		abs	ossif	db ossif	
ant. Inf. iliac spine exostos	abs	>75%			abs	>75%		
acetabulum margin lipping	abs	>10mm			abs	>10mm		
acetabulum post. surface	smth	rough			smth	rough		
acetabulum inf. end lipping	abs	>3mm			abs	>3mm		
isch. tuberosity bumps	abs	<50%	>50%		abs	<50%	>50%	

Sacroiliac Joint	Left				Right			
inferior surface porosity	abs	porosity			abs	porosity		
sup. posterior iliac exostos	smth	exos			smth	exos		
inf. posterior iliac exostos	smth	exos			smth	exos		
posterior exostos	smth	discont	cont		smth	discont	cont	

Pubic Symphysis	Left				Right			
pubic symphyseal collar	abs	collar			abs	collar		
symphyseal relief	billows	resid	flat		billows	resid	flat	
superior protuberance	serrat	knob	flat		serrat	knob	flat	
ventral margin	serrat	ramp	rim	BD	serrat	ramp	rim	BD
dorsal margin	serrat	ramp	rim	BD	serrat	ramp	rim	BD

Collection GURAT	ID# GRAVE HB / GU3

Notes
no auricular surface — some sternal ends
no pubic symphysis — cranial vault preserved

Cranium	Left / Midline				Right		
parietal depression	abs	pres			abs	pres	
spheno-occipital synch.	open	close					
occipital condyle lipping	abs	>50%	>75%		abs	>50%	>75%

Vertebral Column	Midline					
C1 lipping	abs	>50%				
C1 eburnation	abs	pres				
L1 spinuous process	round	flat	ossif			
L1 superior body surface	NF	PF	RL	FF	GF	flat
L1 inferior body surface	NF	PF	RL	FF	GF	flat
L5 superior margin	round	sharp	lipped			
L5 inferior margin	round	sharp	lipped			
L5 superior body surface	NF	PF	RL	FF	GF	flat
L5 inferior body surface	NF	PF	RL	FF	GF	flat
S1 margin	round	sharp	lipped			
S1-2 fusion	>1cm	<1cm	close			
cervical lipping	abs	>3mm			# scorable = 9	
thoracic lipping	abs	>3mm			# scorable = 8	
lumbar lipping	abs	>3mm			# scorable =	
cervical candlewax	abs	pres				
thoracic candlewax	abs	pres				
lumbar candlewax	abs	pres				

Sternum and Ribs	Left / All					Right
sternum dorsal ridge	abs	pres				
R2 rim profile	regular	irreg	abs	cone	claw	both
R3-10 rim profile	regular	irreg	abs	cone	claw	both
R2 shingle rib	norm	shingle				
R3-10 shingle ribs	norm	shingle				

Clavicle / Scapula	Left				Right			
medial epiphysis fusion	NF	PF	RL	FF	NF	PF	RL	FF
medial epiphysis gravel	abs	pres			abs	pres		
medial macroporosity	abs	>3	many		abs	>3	many	
lateral macroporosity	abs	>3			abs	>3		
glenoid fossa lipping	abs	<1/2	>1/2		abs	<1/2	>1/2	

Humerus	Left / All				Right			
humerus weight	normal	light						
lesser tubercle bumps	abs	>1/3			abs	>1/3		
lesser tubercle margin	round	raised	lipped		round	raised	lipped	
greater tubercle pits	abs	pres			abs	pres		
medial epicondyle	smth	rough			smth	rough		
lateral epicondyl	smth	rough			smth	rough		

Trapezium	Left				Right			
trapezium lipping	abs	>2mm			abs	>2mm		

Femur	Left				Right			
fovea margin lipping	abs	>10mm			abs	>10mm		
head surface	smth	>5mm	>10mm		smth	>5mm	>10mm	
gr. trochanter roughening	abs	tri	rec	OH	abs	tri	rec	OH
trochanteric fossa exostos	abs	pres			abs	pres		
trochanteric medial exostos	abs	pres			abs	pres		

Tibia / Fibula / Calcaneus	Left / All				Right			
tibia weight	normal	light			normal	light		
calcaneus weight	normal	light			normal	light		

Inominates	Left / All				Right			
inominate weight	normal	light						
SI joint fusion	abs	fused	SA		abs	fused	SA	
iliac crest fusion	NF	PF	RL	FF	NF	PF	RL	FF
ilium tuberculum ossif	abs	ossif	db ossif		abs	ossif	db ossif	
ant. Inf. iliac spine exostos	abs	>75%			abs	>75%		
acetabulum margin lipping	abs	>10mm			abs	>10mm		
acetabulum post. surface	smth	rough			smth	rough		
acetabulum inf. end lipping	abs	>3mm			abs	>3mm		
isch. tuberosity bumps	abs	<50%	>50%		abs	<50%	>50%	

Sacroiliac Joint	Left				Right			
inferior surface porosity	abs	porosity			abs	porosity		
sup. posterior iliac exostos	smth	exos			smth	exos		
inf. posterior iliac exostos	smth	exos			smth	exos		
posterior exostos	smth	discont	cont		smth	discont	cont	

Pubic Symphysis	Left				Right			
pubic symphyseal collar	abs	collar			abs	collar		
symphyseal relief	billows	resid	flat		billows	resid	flat	
superior protuberance	serrat	knob	flat		serrat	knob	flat	
ventral margin	serrat	ramp	rim	BD	serrat	ramp	rim	BD
dorsal margin	serrat	ramp	rim	BD	serrat	ramp	rim	BD

Collection GURAT ID# GRAVE DC / GU7

Notes:
one mostly intact auricular surface no well preserved sternal ends.
one (and ½) pubic symphyses cranial vault is intact

Cranium	Left / Midline						Right		
parietal depression	abs	pres					abs	pres	
spheno-occipital synch.	open	close							
occipital condyle lipping	abs	>50%	>75%				abs	>50%	>75%

Vertebral Column	Midline					
C1 lipping	abs	>50%				
C1 eburnation	abs	pres				
L1 spinuous process	round	flat	ossif			
L1 superior body surface	NF	PF	RL	FF	GF	flat
L1 inferior body surface	NF	PF	RL	FF	GF	flat
L5 superior margin	round	sharp	lipped			
L5 inferior margin	round	sharp	lipped			
L5 superior body surface	NF	PF	RL	FF	GF	flat
L5 inferior body surface	NF	PF	RL	FF	GF	flat
S1 margin	round	sharp	lipped			
S1-2 fusion	>1cm	<1cm	close			
cervical lipping	abs	>3mm			# Scorable = 0	
thoracic lipping	abs	>3mm			# Scorable = 3	
lumbar lipping	abs	>3mm			# Scorable = 3	
cervical candlewax	abs	pres				
thoracic candlewax	abs	pres				
lumbar candlewax		pres				

Sternum and Ribs	Left / All					Right
sternum dorsal ridge	abs	pres				
R2 rim profile	regular	irreg	abs	cone	claw	both
R3-10 rim profile	regular	irreg	abs	cone	claw	both
R2 shingle rib	norm	shingle				
R3-10 shingle ribs	norm	shingle				

Clavicle / Scapula	Left				Right			
medial epiphysis fusion	NF	PF	RL	FF	NF	PF	RL	FF
medial epiphysis gravel	abs	pres			abs	pres		
medial macroporosity	abs	>3	many		abs	>3	many	
lateral macroporosity	abs	>3			abs	>3		
glenoid fossa lipping	abs	<1/2	>1/2		abs	<1/2	>1/2	

Humerus	Left / All				Right			
humerus weight	normal	light						
lesser tubercle bumps	abs	>1/3			abs	>1/3		
lesser tubercle margin	round	raised	lipped		round	raised	lipped	
greater tubercle pits	abs	pres			abs	pres		
medial epicondyle	smth	rough			smth	rough		
lateral epicondyl	smth	rough			smth	rough		
Trapezium	**Left**				**Right**			
trapezium lipping	abs	>2mm			abs	>2mm		
Femur	**Left**				**Right**			
fovea margin lipping	abs	>10mm			abs	>10mm		
head surface	smth	>5mm	>10mm		smth	>5mm	>10mm	
gr. trochanter roughening	abs	tri	rec	OH	abs	tri	rec	OH
trochanteric fossa exostos	abs	pres			abs	pres		
trochanteric medial exostos	abs	pres			abs	pres		
Tibia / Fibula / Calcaneus	**Left / All**				**Right**			
tibia weight	normal	light			normal	light		
calcaneus weight	normal	light			normal	light		
Inominates	**Left / All**				**Right**			
inominate weight	normal	light						
SI joint fusion	abs	fused	SA		abs	fused	SA	
iliac crest fusion	NF	PF	RL	FF	NF	PF	RL	FF
ilium tuberculum ossif	abs	ossif	db ossif		abs	ossif	db ossif	
ant. Inf. iliac spine exostos	abs	>75%			abs	>75%		
acetabulum margin lipping	abs	>10mm			abs	>10mm		
acetabulum post. surface	smth	rough			smth	rough		
acetabulum inf. end lipping	abs	>3mm			abs	>3mm		
isch. tuberosity bumps	abs	<50%	>50%		abs	<50%	>50%	
Sacroiliac Joint	**Left**				**Right**			
inferior surface porosity	abs	porosity			abs	porosity		
sup. posterior iliac exostos	smth	exos			smth	exos		
inf. posterior iliac exostos	smth	exos			smth	exos		
posterior exostos	smth	discont	cont		smth	discont	cont	
Pubic Symphysis	**Left**				**Right**			
pubic symphyseal collar	abs	collar			abs	collar		
symphyseal relief	billows	resid	flat		billows	resid	flat	
superior protuberance	serrat	knob	flat		serrat	knob	flat	
ventral margin	serrat	ramp	rim	BD	serrat	ramp	rim	BD
dorsal margin	serrat	ramp	rim	BD	serrat	ramp	rim	BD

Collection	GURAT	ID#	GRAVE DC / GU 8

Notes: most of skull vault preserved. R+L auricular surface are present but damaged
no ribs.
no pubic symphysis

Cranium	Left / Midline					Right		
parietal depression	abs	pres				abs	pres	
spheno-occipital synch.	open	close						
occipital condyle lipping	abs	>50%	>75%			abs	>50%	>75%

Vertebral Column	Midline						
C1 lipping	abs	>50%					
C1 eburnation	abs	pres					
L1 spinuous process	round	flat	ossif				
L1 superior body surface	NF	PF	RL	FF	GF	flat	
L1 inferior body surface	NF	PF	RL	FF	GF	flat	
L5 superior margin	round	sharp	lipped				
L5 inferior margin	round	sharp	lipped				
L5 superior body surface	NF	PF	RL	FF	GF	flat	
L5 inferior body surface	NF	PF	RL	FF	GF	flat	
S1 margin	round	sharp	lipped				
S1-2 fusion	>1cm	<1cm	close				
cervical lipping	abs	>3mm		# scorable =			
thoracic lipping	abs	>3mm		# scorable =			
lumbar lipping	abs	>3mm		# scorable =			
cervical candlewax	abs	pres					
thoracic candlewax	abs	pres					
lumbar candlewax	abs	pres					

Sternum and Ribs	Left / All						Right
sternum dorsal ridge	abs	pres					
R2 rim profile	regular	irreg	abs	cone	claw	both	
R3-10 rim profile	regular	irreg	abs	cone	claw	both	
R2 shingle rib	norm	shingle					
R3-10 shingle ribs	norm	shingle					

Clavicle / Scapula	Left				Right			
medial epiphysis fusion	NF	PF	RL	FF	NF	PF	RL	FF
medial epiphysis gravel	abs	pres			abs	pres		
medial macroporosity	abs	>3	many		abs	>3	many	
lateral macroporosity	abs	>3			abs	>3		
glenoid fossa lipping	abs	<1/2	>1/2		abs	<1/2	>1/2	

Humerus	**Left / All**				**Right**			
humerus weight	normal	light						
lesser tubercle bumps	abs	>1/3			abs	>1/3		
lesser tubercle margin	round	raised	lipped		round	raised	lipped	
greater tubercle pits	abs	pres			abs	pres		
medial epicondyle	smth	rough			smth	rough		
lateral epicondyl	smth	rough			smth	rough		
Trapezium	**Left**				**Right**			
trapezium lipping	abs	>2mm			abs	>2mm		
Femur	**Left**				**Right**			
fovea margin lipping	abs	>10mm			abs	>10mm		
head surface	smth	>5mm	>10mm		smth	>5mm	>10mm	
gr. trochanter roughening	abs	tri	rec	OH	abs	tri	rec	OH
trochanteric fossa exostos	abs	pres			abs	pres		
trochanteric medial exostos	abs	pres			abs	pres		
Tibia / Fibula / Calcaneus	**Left / All**				**Right**			
tibia weight	normal	light			normal	light		
calcaneus weight	normal	light			normal	light		
Inominates	**Left / All**				**Right**			
inominate weight	normal	light						
SI joint fusion	abs	fused	SA		abs	fused	SA	
iliac crest fusion	NF	PF	RL	FF	NF	PF	RL	FF
ilium tuberculum ossif	abs	ossif	db ossif		abs	ossif	db ossif	
ant. Inf. iliac spine exostos	abs	>75%			abs	>75%		
acetabulum margin lipping	abs	>10mm			abs	>10mm		
acetabulum post. surface	smth	rough			smth	rough		
acetabulum inf. end lipping	abs	>3mm			abs	>3mm		
isch. tuberosity bumps	abs	<50%	>50%		abs	<50%	>50%	
Sacroiliac Joint	**Left**				**Right**			
inferior surface porosity	abs	porosity			abs	porosity		
sup. posterior iliac exostos	smth	exos			smth	exos		
inf. posterior iliac exostos	smth	exos			smth	exos		
posterior exostos	smth	discont	cont		smth	discont	cont	
Pubic Symphysis	**Left**				**Right**			
pubic symphyseal collar	abs	collar			abs	collar		
symphyseal relief	billows	resid	flat		billows	resid	flat	
superior protuberance	serrat	knob	flat		serrat	knob	flat	
ventral margin	serrat	ramp	rim	BD	serrat	ramp	rim	BD
dorsal margin	serrat	ramp	rim	BD	serrat	ramp	rim	BD

Collection	GURAT	ID#	GRAVE DC / GU 9

Notes: skull vault preserved
no ribs
L auricular surface only
no pubic symphysis

Cranium	Left / Midline					Right			
parietal depression	abs	pres				abs	pres		
spheno-occipital synch.	open	close							
occipital condyle lipping	abs	>50%	>75%			abs	>50%	>75%	

Vertebral Column	Midline					
C1 lipping	abs	>50%				
C1 eburnation	abs	pres				
L1 spinuous process	round	flat	ossif			
L1 superior body surface	NF	PF	RL	FF	GF	flat
L1 inferior body surface	NF	PF	RL	FF	GF	flat
L5 superior margin	round	sharp	lipped			
L5 inferior margin	round	sharp	lipped			
L5 superior body surface	NF	PF	RL	FF	GF	flat
L5 inferior body surface	NF	PF	RL	FF	GF	flat
S1 margin	round	sharp	lipped			
S1-2 fusion	>1cm	<1cm	close			
cervical lipping	abs	>3mm		# scorable =		
thoracic lipping	abs	>3mm		# scorable = 1		
lumbar lipping	abs	>3mm		# scorable = 3		
cervical candlewax	abs	pres				
thoracic candlewax	abs	pres				
lumbar candlewax	abs	pres				

Sternum and Ribs	Left / All					Right
sternum dorsal ridge	abs	pres				
R2 rim profile	regular	irreg	abs	cone	claw	both
R3-10 rim profile	regular	irreg	abs	cone	claw	both
R2 shingle rib	norm	shingle				
R3-10 shingle ribs	norm	shingle				

Clavicle / Scapula	Left				Right			
medial epiphysis fusion	NF	PF	RL	FF	NF	PF	RL	FF
medial epiphysis gravel	abs	pres			abs	pres		
medial macroporosity	abs	>3	many		abs	>3	many	
lateral macroporosity	abs	>3			abs	>3		
glenoid fossa lipping	abs	<1/2	>1/2		abs	<1/2	>1/2	

Humerus	Left / All				Right			
humerus weight	normal	light						
lesser tubercle bumps	**abs**	>1/3			**abs**	>1/3		
lesser tubercle margin	round	**raised**	lipped		**round**	raised	lipped	
greater tubercle pits	abs	pres			abs	pres		
medial epicondyle	smth	rough			**smth**	rough		
lateral epicondyl	smth	rough			**smth**	rough		
Trapezium	Left				Right			
trapezium lipping	abs	>2mm			abs	>2mm		
Femur	Left				Right			
fovea margin lipping	**abs**	>10mm			**abs**	>10mm		
head surface	**smth**	>5mm	>10mm		**smth**	>5mm	>10mm	
gr. trochanter roughening	abs	**tri**	rec	OH	abs	**tri**	rec	OH
trochanteric fossa exostos	abs	**pres**			abs	**pres**		
trochanteric medial exostos	**abs**	pres			**abs**	pres		
Tibia / Fibula / Calcaneus	Left / All				Right			
tibia weight	**normal**	light			normal	light		
calcaneus weight	normal	light			normal	light		
Inominates	Left / All				Right			
inominate weight	normal	light						
SI joint fusion	**abs**	fused	SA		**abs**	fused	SA	
iliac crest fusion	NF	PF	**RL**	FF	NF	PF	RL	FF
ilium tuberculum ossif	**abs**	ossif	db ossif		abs	ossif	db ossif	
ant. Inf. iliac spine exostos	**abs**	>75%			abs	>75%		
acetabulum margin lipping	**abs**	>10mm			abs	>10mm		
acetabulum post. surface	**smth**	rough			**smth**	rough		
acetabulum inf. end lipping	**abs**	>3mm			**abs**	>3mm		
isch. tuberosity bumps	abs	**<50%**	>50%		abs	**<50%**	>50%	
Sacroiliac Joint	Left				Right			
inferior surface porosity	**abs**	porosity			abs	porosity		
sup. posterior iliac exostos	smth	**exos**			smth	exos		
inf. posterior iliac exostos	**smth**	exos			smth	exos		
posterior exostos	**smth**	discont	cont		smth	discont	cont	
Pubic Symphysis	Left				Right			
pubic symphyseal collar	abs	collar			abs	collar		
symphyseal relief	billows	resid	flat		billows	resid	flat	
superior protuberance	serrat	knob	flat		serrat	knob	flat	
ventral margin	serrat	ramp	rim	BD	serrat	ramp	rim	BD
dorsal margin	serrat	ramp	rim	BD	serrat	ramp	rim	BD

Collection GURAT | ID# GRAVE DB / GU 11

Notes: no cranial vault; no ribs; part of L auricular surface intact; no pubic symphysis; HIGHLY FRAG

Cranium	Left / Midline					Right		
parietal depression	abs	pres				abs	pres	
spheno-occipital synch.	open	close						
occipital condyle lipping	abs	>50%	>75%			abs	>50%	>75%

Vertebral Column	Midline					
C1 lipping	abs	>50%				
C1 eburnation	abs	pres				
L1 spinuous process	round	flat	ossif			
L1 superior body surface	NF	PF	RL	FF	GF	flat
L1 inferior body surface	NF	PF	RL	FF	GF	flat
L5 superior margin	round	sharp	lipped			
L5 inferior margin	round	sharp	lipped			
L5 superior body surface	NF	PF	RL	FF	GF	flat
L5 inferior body surface	NF	PF	RL	FF	GF	flat
S1 margin	round	sharp	lipped			
S1-2 fusion	>1cm	<1cm	close			
cervical lipping	abs	>3mm			# Scorable =	
thoracic lipping	abs	>3mm			# Scorable =	
lumbar lipping	abs	>3mm			# scorable =	
cervical candlewax	abs	pres				
thoracic candlewax	abs	pres				
lumbar candlewax	abs	pres				

Sternum and Ribs	Left / All					Right
sternum dorsal ridge	abs	pres				
R2 rim profile	regular	irreg	abs	cone	claw	both
R3-10 rim profile	regular	irreg	abs	cone	claw	both
R2 shingle rib	norm	shingle				
R3-10 shingle ribs	norm	shingle				

Clavicle / Scapula	Left				Right			
medial epiphysis fusion	NF	PF	RL	FF	NF	PF	RL	FF
medial epiphysis gravel	abs	pres			abs	pres		
medial macroporosity	abs	>3	many		abs	>3	many	
lateral macroporosity	abs	>3			abs	>3		
glenoid fossa lipping	abs	<1/2	>1/2		abs	<1/2	>1/2	

Humerus	Left / All				Right			
humerus weight	normal	light						
lesser tubercle bumps	abs	>1/3			abs	>1/3		
lesser tubercle margin	round	raised	lipped		round	raised	lipped	
greater tubercle pits	abs	pres			abs	pres		
medial epicondyle	smth	rough			smth	rough		
lateral epicondyl	smth	rough			smth	rough		

Trapezium	Left				Right			
trapezium lipping	abs	>2mm			abs	>2mm		

Femur	Left				Right			
fovea margin lipping	abs	>10mm			abs	>10mm		
head surface	smth	>5mm	>10mm		smth	>5mm	>10mm	
gr. trochanter roughening	abs	tri	rec	OH	abs	tri	rec	OH
trochanteric fossa exostos	abs	pres			abs	pres		
trochanteric medial exostos	abs	pres			abs	pres		

Tibia / Fibula / Calcaneus	Left / All				Right			
tibia weight	normal	light			normal	light		
calcaneus weight	normal	light			normal	light		

Inominates	Left / All				Right			
inominate weight	normal	light						
SI joint fusion	abs	fused	SA		abs	fused	SA	
iliac crest fusion	NF	PF	RL	FF	NF	PF	RL	FF
ilium tuberculum ossif	abs	ossif	db ossif		abs	ossif	db ossif	
ant. Inf. iliac spine exostos	abs	>75%			abs	>75%		
acetabulum margin lipping	abs	>10mm			abs	>10mm		
acetabulum post. surface	smth	rough			smth	rough		
acetabulum inf. end lipping	abs	>3mm			abs	>3mm		
isch. tuberosity bumps	abs	<50%	>50%		abs	<50%	>50%	

Sacroiliac Joint	Left				Right			
inferior surface porosity	abs	porosity			abs	porosity		
sup. posterior iliac exostos	smth	exos			smth	exos		
inf. posterior iliac exostos	smth	exos			smth	exos		
posterior exostos	smth	discont	cont		smth	discont	cont	

Pubic Symphysis	Left				Right			
pubic symphyseal collar	abs	collar			abs	collar		
symphyseal relief	billows	resid	flat		billows	resid	flat	
superior protuberance	serrat	knob	flat		serrat	knob	flat	
ventral margin	serrat	ramp	rim	BD	serrat	ramp	rim	BD
dorsal margin	serrat	ramp	rim	BD	serrat	ramp	rim	BD

Collection	GURAT	ID#	GRAVE DB / GU 12

Notes
no ribs — no auricular surface — HIGHLY FRAG.
no skull vault — no pubic symphyses

Cranium	Left / Midline						Right			
parietal depression	abs	pres					abs	pres		
spheno-occipital synch.	open	close								
occipital condyle lipping	abs	>50%	>75%				abs	>50%	>75%	

Vertebral Column	Midline					
C1 lipping	abs	>50%				
C1 eburnation	abs	pres				
L1 spinuous process	round	flat	ossif			
L1 superior body surface	NF	PF	RL	FF	GF	flat
L1 inferior body surface	NF	PF	RL	FF	GF	flat
L5 superior margin	round	sharp	lipped			
L5 inferior margin	round	sharp	lipped			
L5 superior body surface	NF	PF	RL	FF	GF	flat
L5 inferior body surface	NF	PF	RL	FF	GF	flat
S1 margin	round	sharp	lipped			
S1-2 fusion	>1cm	<1cm	close			
cervical lipping	abs	>3mm			# Scorable =	
thoracic lipping	abs	>3mm			# Scorable =	
lumbar lipping	abs	>3mm			# Scorable =	
cervical candlewax	abs	pres				
thoracic candlewax	abs	pres				
lumbar candlewax	abs	pres				

Sternum and Ribs	Left / All						Right
sternum dorsal ridge	abs	pres					
R2 rim profile	regular	irreg	abs	cone	claw	both	
R3-10 rim profile	regular	irreg	abs	cone	claw	both	
R2 shingle rib	norm	shingle					
R3-10 shingle ribs	norm	shingle					

Clavicle / Scapula	Left				Right			
medial epiphysis fusion	NF	PF	RL	FF	NF	PF	RL	FF
medial epiphysis gravel	abs	pres			abs	pres		
medial macroporosity	abs	>3	many		abs	>3	many	
lateral macroporosity	abs	>3			abs	>3		
glenoid fossa lipping	abs	<1/2	>1/2		abs	<1/2	>1/2	

Humerus	**Left / All**				**Right**			
humerus weight	normal	light						
lesser tubercle bumps	abs	>1/3			abs	>1/3		
lesser tubercle margin	round	raised	lipped		round	raised	lipped	
greater tubercle pits	abs	pres			abs	pres		
medial epicondyle	smth	rough			smth	rough		
lateral epicondyl	smth	rough			smth	rough		
Trapezium	**Left**				**Right**			
trapezium lipping	abs	>2mm			abs	>2mm		
Femur	**Left**				**Right**			
fovea margin lipping	abs	>10mm			abs	>10mm		
head surface	smth	>5mm	>10mm		smth	>5mm	>10mm	
gr. trochanter roughening	abs	tri	rec	OH	abs	tri	rec	OH
trochanteric fossa exostos	abs	pres			abs	pres		
trochanteric medial exostos	abs	pres			abs	pres		
Tibia / Fibula / Calcaneus	**Left / All**				**Right**			
tibia weight	normal	light			normal	light		
calcaneus weight	normal	light			normal	light		
Inominates	**Left / All**				**Right**			
inominate weight	normal	light						
SI joint fusion	abs	fused	SA		abs	fused	SA	
iliac crest fusion	NF	PF	RL	FF	NF	PF	RL	FF
ilium tuberculum ossif	abs	ossif	db ossif		abs	ossif	db ossif	
ant. Inf. iliac spine exostos	abs	>75%			abs	>75%		
acetabulum margin lipping	abs	>10mm			abs	>10mm		
acetabulum post. surface	smth	rough			smth	rough		
acetabulum inf. end lipping	abs	>3mm			abs	>3mm		
isch. tuberosity bumps	abs	<50%	>50%		abs	<50%	>50%	
Sacroiliac Joint	**Left**				**Right**			
inferior surface porosity	abs	porosity			abs	porosity		
sup. posterior iliac exostos	smth	exos			smth	exos		
inf. posterior iliac exostos	smth	exos			smth	exos		
posterior exostos	smth	discont	cont		smth	discont	cont	
Pubic Symphysis	**Left**				**Right**			
pubic symphyseal collar	abs	collar			abs	collar		
symphyseal relief	billows	resid	flat		billows	resid	flat	
superior protuberance	serrat	knob	flat		serrat	knob	flat	
ventral margin	serrat	ramp	rim	BD	serrat	ramp	rim	BD
dorsal margin	serrat	ramp	rim	BD	serrat	ramp	rim	BD

Appendix B:
Traditional Age-at-Death Scoring Done Using the Buikstra & Ubelaker (1994) Standards

Buckberry & Chamberlain Auricular Surface

ID	**Auricular Surface Phase**		**Age Estimation**
	L	R	
GU 1	4	5	35-44
GU 2	5	4	35-44
GU 3	—	—	
GU 7	7	5	40-59
GU 8	4	—	35-39
GU 9	6	—	45-49
GU 11	6	—	45-49
GU 12	—	—	

Suchey-Brooks Pubic Symphysis

ID	**Suchey-Brooks Phase**		**Age Estimation**
	L	R	
GU 1	—	—	
GU 2	4	3	21-57
GU 3	—	—	
GU 7	5	3	21-66
GU 8	—	—	
GU 9	—	—	
GU 11	—	—	
GU 12	—	—	

Meindl & Lovejoy Cranial Sutures

	Vault		*Lateral-Anterior*	
ID	**Score**	**Age**	**Score**	**Age**
GU 1	n/a		n/a	
GU 2	8	27-44	11	29-54
GU 3	3*	22-45*	5*	28-51*
GU 7	11	27-44	13	29-54
GU 8	7*	27-44	n/a	
GU 9	1	18-43	n/a	
GU 11	n/a		n/a	
GU 12	n/a		n/a	

*not all sutures in the region could be scored

Age Classifications from Results of Traditional Age-at-Death Analysis

ID	**Classification**
GU 1	Middle Adult
GU 2	Middle Adult
GU 3	Young Adult
GU 7	Middle Adult
GU 8	Middle Adult
GU 9	Middle Adult
GU 11	Middle Adult
GU 12	n/a

Appendix C:
Photographs of the Gurat Skeletal Collection

GU 1

Pelvis

Partial S1-S2 fusion

GU 2

Pelvis

Pubic symphysis

GU 3

Pelvis

Sternal end of the clavicle (partially fused)

GU 7

Pelvis


Candlewax on a lumbar vertebra

GU 8

Pelvis

GU 9

Pelvis

Trochanteric fossa exostoses

GU 11

Pelvis

Fovea margin lipping

GU 12

Pelvis